Computational Brain & Behavior (2021) 4:70–86
https://doi.org/10.1007/s42113-020-00076-w

ORIGINAL PAPER

# Hierarchical Hidden Markov Models for Response Time Data

Deborah Kunkel[1] · Zhifei Yan[2] · Peter F. Craigmile[2] · Mario Peruggia[2] · Trisha Van Zandt[2,3]

Published online: 26 March 2020
© Society for Mathematical Psychology 2020

## Abstract

Psychological data, particularly measurements obtained sequentially in experiments designed to test theories of human cognition, are often treated as independent and identically distributed samples from a single distribution that describes the cognitive process. This assumption is made for mathematical and analytic convenience; it is widely appreciated that such data are in fact mixtures from two or more processes, only a subset of which are associated with the cognitive process of interest. Our modeling framework describes response times (RTs) as arising from a mixture of three distinct distributions. Transitions across the distributions are governed by a hidden Markov structure whose states produce either fast, average, or slow RTs. This process is nested within a second hidden Markov structure, producing an "environment" process that allows the distribution of the response modes to evolve due to both internal factors (such as fatigue and distractions) and external factors (such as changing task demands). We performed a detection experiment designed to elicit responses under three environments that mimic external conditions that influence latent response modes. We present our hierarchical model and demonstrate its fit on the experimental data. We also demonstrate the model's fit in the case when external conditions were not manipulated as part of the experimental process.

**Keywords** Bayesian modeling · Cognitive modeling · Mixture distributions · Transition probabilities

## Introduction

Psychological data, particularly those measurements obtained sequentially in experiments designed to test theories and models of human cognition, are often treated as independent and identically distributed (i.i.d.) samples from a single distribution that describes the random behavior of a cognitive process. This assumption is made for mathematical and analytic convenience; it is more realistic to assume that several processes may contribute to a given sequence of measurements. In cognitive models which posit two or more processes, it is natural to assume the existence of discrete latent variables, each of which corresponds to a distinct data-generating mechanism, and which together produce a mixture distribution for the data.

The mixture construct has been an important tool in many areas, including the investigation of memory phenomena such as spreading activation and response preparation (e.g., Meyer et al. 1988; Yantis and Meyer 1988), the identification of contaminant observations from a data set (Vandekerckhove et al. 2008), and the distinction between on-task and mind-wandering behaviors (Smallwood and Schooler 2015; Hawkins et al. 2017). Our own work (Craigmile et al. 2010; Kim et al. 2017) has demonstrated the importance of including components to describe fast (*subcognitive*) and slow (*supracognitive*) processes in addition to the cognitive process that corresponds to an attentive performance of the task.

It is important to distinguish between the processes that produce different kinds of responses and the environments in which the processes are operating. Some environments will promote more of one kind of response than others, and so the environment will determine the probabilities of responses from the different mixture components. Changes in that environment may result in modified behavior that lasts for several consecutive trials. For example, periods of intense focus may promote responses from a single cognitive process, and the RTs would arise from a single distribution with little variability over other mixture components.

**Electronic supplementary material** The online version of this article (https://doi.org/10.1007/s42113-020-00076-w) contains supplementary material, which is available to authorized users.

✉ Deborah Kunkel
dekunke@clemson.edu

[1] School of Mathematical and Statistical Sciences, Clemson University, Clemson, SC 29634, USA

[2] Department of Statistics, The Ohio State University, Columbus, OH 43210, USA

[3] Department of Psychology, The Ohio State University, Columbus, OH 43210, USA

Conversely, a state of fatigue may lead to frequent too-slow and too-fast responses.

The assumption that the latent variables corresponding to the mixture components are i.i.d. permits the mixture model to capture sporadic, momentary location shifts in RT distributions but not long-term changes in behavior. This fact motivates a modeling approach that captures these patterns through a single, flexible latent process that incorporates both the mixture components and the external or internal environments in which the psychological processes operate. In this article, we build on classic studies that attempt to distinguish the separate latent components of a psychological mixture process (Falmagne 1965; Ollman 1966; Falmagne 1968; Yellott 1971; Lindsen and de Jong 2010; Molenaar and Boeck 2018; Ranger et al. 2018). Our modeling framework uses a hidden Markov structure with a two-dimensional latent state, which accounts for both short- and long-term location and concentration changes in RT distributions and provides a flexible representation of periods of trials in which a person's behavior is stable.

Our framework is a hidden Markov model (HMM). A HMM defines the distribution of an observable sequence of measurements $\{y_t : t = 1, \ldots, T\}$ that depends on a second unobserved sequence $\{s_t : t = 1, \ldots, T\}$ of discrete random variables. The variable $s_t$ is the *state* of the process at time $t$. A different value for the state $s_t$ generates a different probability distribution for $y_t$. The sequence of these hidden states is a *Markov chain*, where the probability of moving to a particular state at the next time point depends on the history of the sequence only through the value of the current state. This statistical model on states $\{s_t\}$ allows for dependence among the observations $\{y_t\}$ while also permitting inferences to be made about the distribution of the underlying states that generate changes in the observations' distribution.

HMMs have been used with great success in many applications where data are thought to be tied to an underlying hidden structure that might change over the span of the sequence. In addition to cognitive models, where the latent states correspond to mental states such as mind-wandering (Bastian and Sackur 2013) and stages of information processing (Borst and Anderson 2015), HMMs are popular tools in a diverse set of disciplines. In economics, a hidden state may represent an underlying state of economic volatility that drives times series of economic indicators (e.g., Bhar and Hamori 2004). Popular decoding algorithms in computational biology use HMMs to parse observed DNA sequences into coding regions or stop/start sequences (e.g., Wang et al. 2004; Majoros 2007; Yoon 2009). Sarkar et al. (2018) use an HMM with covariate-dependent transition probabilities to induce a semiparametric structure. In speech recognition and synthesis, the hidden Markov model has been a standard tool for analysis for several decades (e.g., Gales and Young 2007; Tokuda et al. 2013). Rabiner (1989) and Juang and Rabiner (1991) describe some commonly used HMMs for speech analysis. For example, *isolated word recognition* builds a distinct statistical model for each word using a hidden sequence of phoneme states to generate the observed sound sequence; coarser components of language, such as sentences and phrases are similarly modeled using additional, nested, HMMs.

The latent state in our proposed hidden Markov model comprises two elements. The first indicates the process that is active as a given measurement is generated. The second (*an environment*) represents a changing condition which could correspond to external or internal factors, such as task set or level of fatigue, that makes responses from certain processes more or less likely. The Markov property of the hidden states allows latent states to persist over trials, to a possibly varying degree for different people.

We conducted an experiment in which we manipulated the experimental conditions to promote responses from different RT distributions, mimicking those internal or external mental states whose periodic changes may cause changes in response speed or behavioral variability. Because our model captures variability across individuals, we explore the person-specific HMM mechanisms as represented by their unique transition probabilities across environments and response modes. We describe our experimental procedure in "The Experiment." In "A Bayesian Hierarchical HMM for RTs," we present our model. In "Results," we present the results of fitting our model to the experimental data. In "Model Validation," we assess how our model fits our experimental data, and also present the results of fitting our model to data from another experiment in which environmental conditions were not manipulated. We close with a discussion of additional potential applications of this modeling framework in "Conclusions and Discussion."

## The Experiment

We conducted an experiment with the goal of creating three experimental conditions that promote RTs from three distinct probability distributions. Each condition established a different task set which corresponded to different environments. Within each environment, we expected to see extended periods of fast, medium, or slow RTs. Participants were told they were commanding a spaceship and instructed to press a space bar ("destroy an enemy ship") when a small target appeared on the computer monitor. They were given a visual shield that indicated the position of their own ship and when they were visible or invisible to the enemy ship. Destroying the enemy ship when invisible was sub-optimal (although possible), because they could implement repairs to their own ship without risk; failing to destroy the enemy ship when visible was sub-

optimal (although possible), because the enemy ship would begin to fire and gradually deteriorate the integrity of the participant's own ship.

To implement the different environments, the location of the participant's ship behind the shield (and the shield color) was varied so that it was either very close, farther, or very far from the shield boundary. Because of the tradeoff between ship repair time and ship damage from being fired upon, the optimal strategy was to time the keypress that destroyed the enemy ship for the moment that the participant's own ship emerged from behind the shield. The purpose of this design was to first mimic patterns of movement between latent mental states, and to second ensure that, regardless of the task set, a participant was still able to select responses that were either very fast, slower, or very slow, as s/he felt so compelled.

We chose this design to ensure complete control over the environments in the experiment. While we might have chosen to implement experimental variables that mimicked some possible number of mental states (focused vs. unfocused attention or fatigued vs. rested, for example), even in the most meticulously designed experiment we would never be certain what an individual's true mental state was. This design will produce data similar to RT data obtained from mixtures over response processes (e.g., guessing, distraction, or focused task performance) under different latent mental states. We purposefully ignored the experimental condition (stimulus distance) in our modeling to mimic the real-world research problem of never knowing a participant's latent mental state.

**Participants** Fifty-six students were recruited from the Ohio State University Department of Psychology's Research Experience Program pool. All students were naive to the purposes of the experiment and reported normal or corrected-to-normal vision. Of the 56 students, 13 did not finish, choosing either to leave the experiment early or simply stopped performing the task. The data from these 13 students were eliminated, leaving data from 43students for analysis.

**Materials and Procedures** The software that presented the stimuli and recorded responses was programmed in Python using Sederberg's (2016) SMILE library (https://github.com/compmem/smile/). Using this library, RTs were measured to within 8 ms accuracy. The code is included in the supplementary materials.

Participants were welcomed to the experiment with a description of the task they were to perform (Fig. 1). A transparent circular aperture (the shield) appeared on the computer monitor and moved continuously following a two-dimensional Brownian motion process within a restricted square region on the screen. The aperture was superimposed on an expanding random particle field that simulated a "starfield," and the expansion simulated forward movement of the aperture through the field. At random intervals, a small

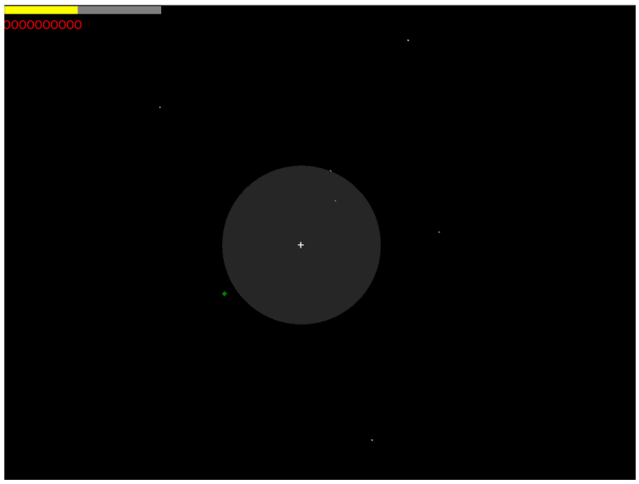

**Fig. 1** An example of the experimental task

green circular target (the enemy ship) appeared in the aperture and immediately began moving toward the aperture boundary along the straight-line trajectory of minimum distance. The participant's task was to press the space bar on the computer keyboard after the target was detected to destroy it.

The condition of the participant's ship was presented as a horizontal bar in the upper left-hand corner of the screen. The bar varied in color as the condition of the starship improved or deteriorated. If the condition bar reached zero, it was destroyed and the participant lost a life. The number of lives remaining was presented as a string of red "O" characters just below the starship condition bar. Participants began the experiment with 10 lives.

The rate at which the ship's condition improved while the target was contained in the aperture was two orders of magnitude smaller than the rate at which the ship condition deteriorated when the target moved outside the aperture. Therefore, it was to the participant's advantage to withhold a response until the instant that the target reached the aperture boundary.

The aperture had a radius of 100 pixels, and the target could appear at a random angle (from 0 to 359°) either 85, 90, or 99 pixels from the aperture center. Each distance condition was signaled by a change in the aperture color: for blue, gray, or red apertures the target appeared 85, 90 and 99 pixels from the center, respectively. The aperture color was determined by a Markov chain, in which the probability that the aperture would change color on any target presentation was 0.15, and the probability that the aperture would stay the same color was 0.85. If the aperture changed color, it changed to one of the two other colors with equal probability.

On successive trials, the target appeared at a random interval following the end of the previous trial. This interval was determined in part by an exponential random variable with mean 200 ms. Following the participant's response to the target, the target "exploded" by changing to red and increasing its diameter, a process that took 250 ms. The target explosion,

starfield presentation, and aperture movement added an additional, approximately normally distributed, delay to the response-stimulus interval that had a mean of 1.38 s and a standard deviation of 0.28 s. Remaining details about stimulus timing, sizes, and so forth can be found in the experiment code, which is available in the supplementary materials.

Each participant performed 25 practice trials for which the aperture cycled through all three colors. After these practice trials, the ship condition and number of lives were reset, and the participant performed 820 trials with no rest breaks. After these trials were completed, the participant was debriefed.

## A Bayesian Hierarchical HMM for RTs

Our methodological objective is to establish a principled framework for discovering and modeling possible hidden environments and response modes that influence the distributional characteristics of the observed RTs.

We postulate the existence of three distinct RT distributions and we introduce latent response modes that correspond to these distributions. A person in response mode 1 at trial $t$ will generate fast RTs from the fast process. A person in response mode 2 at trial $t$ will generate medium-length RTs and a person in response mode 3 at trial $t$ will generate slow RTs. These three distributions may represent three modes of performance in a task, as in our experiment, or they may indicate responses from subcognitive, cognitive, and supracognitive processes.

We further posit the existence of several latent environments, each of which causes people to transition differently among the latent response modes. In practical applications, as the name suggests, these latent environments may relate to external, unmeasured background conditions and circumstances influencing a person's performance, such as learning and fatigue. The experiment described in "The Experiment" produces useful test data for the proposed modeling framework because the distance of the target to the ship affects the timing of the task, and thus, the nature of the observed RTs. The three distances from the aperture boundary (85, 90 and 99 pixels) elicit periods of slow, moderate, and fast responses that mimic the unmeasured environmental effects we expect to see in practice. Rather than specifying an RT model that directly relates RT to distance, we use three latent environments to accommodate the shifts in RT distributions. (Note that in most situations, we would not have knowledge of how many environments there are and would have to select their number on the basis of substantive modeling considerations. In "Application to Wagenmakers' data," we demonstrate that our three-environment model can be successfully applied to data from experiments where there were no changes in the task environment, and so determine the extent to which experiment participants moved between different latent states.)

Our model has two key features. First, (i) each environment promotes transitions to a favored latent response mode. Conditional on being in environment $i$ at trial $t$, a person will be in response mode $i$ with high probability at trial $t + 1$ regardless of the response mode in which he or she was at trial $t$. Second, (ii) we assume a certain "stickiness" of the environments: a person in environment $i$ at trial $t$ is likely to remain in environment $i$ at trial $t + 1$. It is this sticky property of the environments that allows them to capture behavior in periods of adjacent trials where external conditions are similar.

### A Markov Process for Response Modes and Environments

We model the sequence of latent environments and response modes as a hidden Markov chain with nine states $(e, r)$, $e, r \in \{1, 2, 3\}$, where the first coordinate, $e$, represents environment and the second coordinate, $r$, represents response mode. The transition probability matrix (TPM) of the Markov chain is a 9 × 9 matrix whose rows and columns are indexed by pairs of environments and response modes (see Fig. 2 for an example of the indexing). Then, the TPM entry indexed by row pair $(i, j)$, and column pair $(k, l)$ contains the probability of transitioning into state $(k, l)$ (environment $k$ and response mode $l$) at time $t + 1$ conditional on being in state $(i, j)$ (environment $i$ and response mode $j$) at time $t$. We assume a conditional structure for the transitions between response modes given environments that allows us to write the probability of transitioning from $(e_t, r_t) = (i, j)$ to $(e_{t+1}, r_{t+1}) = (k, l)$ as

$$P[(e_{t+1}, r_{t+1}) = (k, l) \mid (e_t, r_t) = (i, j)] = P[r_{t+1} = l \mid (e_t, r_t) = (i, j)]\, P[e_{t+1} = k \mid e_t = i]. \quad (1)$$

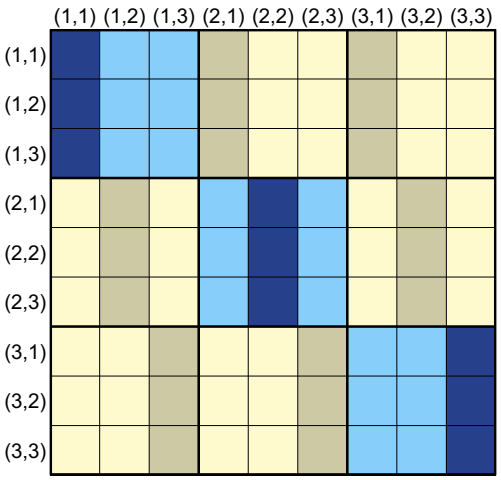


**Fig. 2** Qualitative structure of the expected prior transition probability matrix for the hidden states. The state corresponding to environment $e$ and response mode $r$ is labeled $(e,r)$. Blue represents large probabilities and tan represents small probabilities, with darker shades representing larger probabilities within either color

With this representation we can specify the full 9 × 9 TPM of the hidden Markov chain using $\boldsymbol{Q}$, a 3 × 3 matrix that specifies transition probabilities among the environments, and $\boldsymbol{P}^1$, $\boldsymbol{P}^2$, and $\boldsymbol{P}^3$, a set of 3 × 3 matrices that specify transition probabilities among the response modes conditional on being in environment 1, 2, and 3, respectively. The $(i, k)$th element of $\boldsymbol{Q}$ is $P[e_{t+1} = k \mid e_t = i]$. The $(j, l)$th element of $\boldsymbol{P}^e$ is $P[r_{t+1} = l \mid (e_t, r_t) = (e, j)]$, for $e = 1, 2, 3$.

We incorporate the desired qualitative features of the latent process via an appropriate prior specification of the TPM. The desideratum (i) that each environment favor a particular response mode translates into the requirement that $P[r_{t+1} = l \mid (e_t, r_t) = (i, j)]$ be large when $l = i$ and small otherwise. The desideratum (ii) of "sticky" environments requires that $P[e_{t+1} = k \mid e_t = i]$ be large when $k = i$ and small otherwise. This structure of the expected TPM is described visually in Fig. 2, where, qualitatively, blue represents large probabilities and tan represents small probabilities, with darker shades representing larger probabilities within either color. The fact that the three blue blocks line up along the main diagonal captures desideratum (ii) (the "stickiness of environments"). Desideratum (i) (that each enviroment favors a latent response mode) is captured by the fact that each of the three blocks in the top row has higher probabilities in the first column, each of the three blocks in the middle row has higher probabilities in the second column, and each of the three blocks in the bottom row has higher probabilities in the third column. We describe the models for the TPMs in detail in "Modeling the TPMs."

## Modeling the TPMs

**Model for $\boldsymbol{Q}$** We assume that the environment process differs across people and we introduce an additional subscript in our notation: let $e_{i,t}$ denote the environment for person $i$ at trial number $t$. Then, person $i$'s conditional probability of transitioning to environment $e$ ($e = 1, 2, 3$) at trial $t + 1$ given the current environment $d$ ($d = 1, 2, 3$) at trial $t$ is

$$P\left(e_{i,t+1} = e | e_{i,t} = d\right) = \boldsymbol{Q}_{de}^{(i)}. \tag{2}$$

Each row $d = 1, 2, 3$ of the TPM tabulates the probability of transitioning from the current environment $d$ to one of the environments in columns $e$ ($e = 1, 2, 3$) at the next step. As we have exhaustive conditional probabilities, each row of the matrix $\boldsymbol{Q}^{(i)}$ must sum to 1; i.e., $\sum_{e=1}^{3} \boldsymbol{Q}_{de}^{(i)} = 1$ for each $d$.

The prior distribution of the environment transition matrix $\boldsymbol{Q}^{(i)}$ is the same across people. We assume an expected prior probability of 0.9 of staying in the current environment and an expected prior probability of 0.05 of moving to either one of the other environments. Assuming that row $j$ of $\boldsymbol{Q}^{(i)}$ has a Dirichlet distribution with parameter $\pi_j$ and is independent of the other rows, we guarantee the above expected prior probabilities by setting

$$\begin{aligned} \pi_1 &= (9, 0.5, 0.5); \\ \pi_2 &= (0.5, 9, 0.5); \\ \pi_3 &= (0.5, 0.5, 9). \end{aligned} \tag{3}$$

(Specifications proportional to these parameter values would result in priors with the same expected probabilities but different concentrations.)

**Model for $\boldsymbol{P}^e$, $e = 1, 2, 3$** The notation $r_{i,t}$ denotes one of the three response modes in which person $i$ is at the current trial $t$: 1: fast, 2: medium, or 3: slow.

Applying the decomposition in (1), given that person $i$ is currently in environment $e_{i,t} = e$, we denote the probability of transitioning from the current response mode $r_{i,t} = r$ to response mode $r_{i,t+1} = s$ by

$$\boldsymbol{P}_{rs}^{(i,e)} = P\left(r_{i,t+1} = s | r_{i,t} = r, e_{i,t} = e\right). \tag{4}$$

For each person $i$, these conditional transition probabilities are arranged in three 3 × 3 matrices $\boldsymbol{P}^{(i,e)}$. We place high prior probability on transitions to the response mode that matches the current environment by assuming that each row of $\boldsymbol{P}^{(i,e)}$ has an independent, identical Dirichlet distribution with parameter $\pi_e$ as defined in (5) below. This promotes a prior expectation that transitions to response mode $e$ will be highly likely when the person is in environment $e$. The prior expectations of $\boldsymbol{P}^{(i,e)}$, $e = 1, 2, 3$, are

$$E\left(\boldsymbol{P}^{(i,1)}\right) = \begin{bmatrix} 0.90 & 0.05 & 0.05 \\ 0.90 & 0.05 & 0.05 \\ 0.90 & 0.05 & 0.05 \end{bmatrix}, \quad E\left(\boldsymbol{P}^{(i,2)}\right) = \begin{bmatrix} 0.05 & 0.90 & 0.05 \\ 0.05 & 0.90 & 0.05 \\ 0.05 & 0.90 & 0.05 \end{bmatrix}, \text{ and}$$

$$E\left(\boldsymbol{P}^{(i,3)}\right) = \begin{bmatrix} 0.05 & 0.05 & 0.90 \\ 0.05 & 0.05 & 0.90 \\ 0.05 & 0.05 & 0.90 \end{bmatrix}. \tag{5}$$

## Modeling the RTs

We model the RTs for a given person as arising from one of three Weibull distributions, where each distribution corresponds to one of the latent response modes. The Weibull distribution was proposed as a probabilistic model for RT data by Logan (1988, 1992), who introduced "Instance Theory," a theory of skill acquisition in which memory traces of correct responses to different stimuli race against each other to be retrieved. While this distribution does not perfectly describe the distribution of RT data from every experiment, it does provide a convenient framework for building hierarchical models for RT data (e.g., Peruggia et al. 2002; Rouder et al. 2003, 2005; Craigmile et al. 2012).

In general, a positive random variable $W$ follows a Weibull($\beta$, $\lambda$) distribution with shape parameter $\beta > 0$ and scale parameter $\lambda > 0$ if its cumulative distribution function is

$$F_W(w) = 1-\exp\left(-\left(\frac{w}{\lambda}\right)^{\beta}\right), \quad w > 0.$$

When $\beta = 1$, we have an exponential distribution.

Let $Y_{i,t}$ denote the RT for person $i$ and trial $t$. We assume that the RT distribution depends on the response mode $r_{i,\,t}$ through

$$Y_{i,t}|r_{i,t} = r \sim \text{Weibull}(\beta_i, \lambda_i(r)). \tag{6}$$

In line with other work in this field, we assume that the shape parameter is constant over the trials, but the scale depends on the latent cognitive response mode (Logan 1992; Palmer et al. 2011). We allow both parameters to vary across individuals. Thus, in Eq. (6), we assume that the shape parameter $\beta_i$ depends only on the person $i$, but that the scale parameter $\lambda_i(r_{i,t})$ depends on the person and the hidden response mode $r_{i,t}$. Note that for a fixed shape parameter, as the scale parameter increases the mean and variance of the RT increase (see Craigmile et al. 2012, for further details.)

### Priors for the Weibull Parameters

We specify a model where the scale parameters $\lambda_i(r_{i,t})$ depend on the response modes $r_{i,t}$ and are distributionally tied together in a Bayesian hierarchy that enables sharing of information across people. For each person $i$ and response mode $r$ we assume that the log scale, log $\lambda_i(r)$, has a normal distribution with a person-specific mean $\mu_i^{(r)}$ and standard deviation $\sigma_\lambda^{(r)}$. Both of these parameters depend on the response mode $r$, because we believe that the distributions of the RT scales should change depending on whether a person is in the slow, medium, or fast response mode.

To promote stochastic ordering among the distributions of the log scales for the three response modes we assume that their means are ordered and specify a trivariate constrained normal distribution for $\boldsymbol{\mu}_i = \left(\mu_i^{(1)}, \mu_i^{(2)}, \mu_i^{(3)}\right)^T$:

$$\boldsymbol{\mu}_i \sim N_3(\boldsymbol{\mu}, \Sigma)\, I\left(\mu_i^{(1)} < \mu_i^{(2)} < \mu_i^{(3)}\right),$$

where $\boldsymbol{\mu} = (\mu^{(1)}, \mu^{(2)}, \mu^{(3)})^T$ denotes the mean vector, $\Sigma$ denotes the covariance matrix, and $I(\cdot)$ denotes the indicator function. Note that this model does not postulate that the scales $\lambda_i(r_{i,t})$ are ordered as a function of response mode, only that their means are ordered. The covariance matrix $\Sigma$ is assumed to be a 3 × 3 diagonal matrix whose $r$th diagonal element is $\sigma_\mu^{(r)}$.

The population-level mean vector of the log scales, $\boldsymbol{\mu}$, has a trivariate normal distribution with mean $\boldsymbol{\kappa} = (6, 7, 8)^T$ and covariance matrix $\boldsymbol{V}$, constrained to the region where $\mu^{(1)} < \mu^{(2)} < \mu^{(3)}$. We assume that $\boldsymbol{V}$ is a diagonal matrix with diagonal elements all equal to 0.1.

For the shape parameter of the Weibull distribution for person $i$, we assume that log $\beta_i$ has a normal distribution with mean 2 and standard deviation 0.3. We give the response mode-specific standard deviations of the log scale parameters $\sigma_\lambda^r$ and the response mode-specific standard deviations of the $\mu_i^{(r)}$ half-Cauchy distributions with scale parameter 0.5. (The half-Cauchy distribution is commonly used as a prior for random effect variances; see Gelman 2007, for details.)

We assume that these prior distributions are mutually conditionally independent of one another and across people.

## Results

We fit the model in R using a forward-backward MCMC algorithm (Frühwirth-Schnatter 2006) whose details are described in the supplementary materials. In this section, we use the posterior estimates of the model parameters to characterize the distinct RT distributions in each response mode and to characterize the TPMs that govern each person's transitions among environments and response modes.

### Characterization of the RT Distributions

A key feature of our model is the assumption of three distinct Weibull distributions corresponding to response modes 1, 2, and 3. At the population level, the parameter $\boldsymbol{\mu} = (\mu^{(1)}, \mu^{(2)}, \mu^{(3)})^T$ distinguishes the mean log scales among the three response modes.

Samples from the posterior and prior distributions of $\mu^{(1)}$, $\mu^{(2)}$, and $\mu^{(3)}$ are shown in the left panel of Fig. 3, with the left boxplot for each response mode showing samples from the prior distribution and the right boxplot showing samples from the posterior. The posterior distributions are more concentrated and have smaller means than the prior, producing predictive RT distributions that, in each response mode, concentrate the bulk of their mass on somewhat faster responses. This is illustrated by a comparison of the middle and right panels of Fig. 3 which show Monte Carlo estimates of the predictive densities based on the prior (middle) and posterior (right) distributions of the hyperparameters. (Note that these densities ignore the additional person-to-person variability in the RT distributions.) Also, a posteriori, there is increased separation between the RT distributions for the three response modes.

Individuals are allowed to deviate from the population-level model through the person-specific log scale and log shape parameters. Figure 4 shows Monte Carlo estimates of the three predictive RT densities based on posterior samples for participants 38, 39, 55, and 59. These participants are labeled A, B, C, and D, respectively, and will be referred to by those labels for the remainder of this section. From the figure, we learn that participants B and C have RT

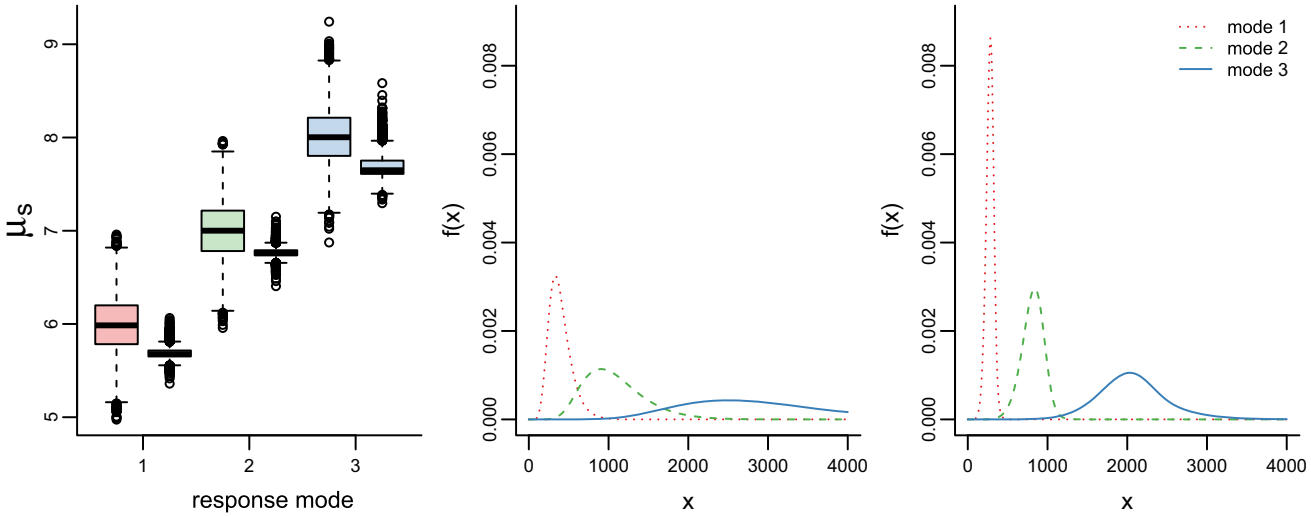


**Fig. 3** The left panel displays boxplots summarizing the prior and posterior distributions of $\mu^{(r)}$ for response mode r = 1 (red), 2 (green), and 3 (blue). For each response mode, the left boxplot is the prior distribution and the right boxplot is the posterior distribution. The middle panel shows predictive densities for each response mode based on the samples from the prior distributions, and the right panel shows predictive densities for each response mode based on the samples from the posterior distributions, ignoring person-specific variability

distributions for the three response modes that produce faster RTs than those of the other two people. The RT distributions for participant D produce unusually slow RTs in all three response modes; in particular, the slow response mode produces very slow responses.

## Characterization of the Latent Process

The latent process that produces changes in person *i*'s RT distributions is governed by the transition matrices $\boldsymbol{Q}^{(i)}$ and $\boldsymbol{P}^{(i,1)}$, $\boldsymbol{P}^{(i,2)}$, $\boldsymbol{P}^{(i,3)}$. The prior information in our model reflects the hypothesized evolution of each person's latent process: the prior on $\boldsymbol{Q}^{(i)}$ places high probability on the diagonal elements, encouraging the environment to persist over consecutive trials, while the priors on $\boldsymbol{P}^{(i,e)}$, $e$ = 1, 2, 3 promote transitions to response mode $e$ whenever the person is in environment $e$. We summarize the posterior distribution of these matrices for person $i$ using Monte Carlo estimates of their posterior means, which we denote by $\bar{\boldsymbol{Q}}^{(i)}$ and $\bar{\boldsymbol{P}}^{(i,e)}$, $e$ = 1, 2, 3.

**Transitions Among Environments** Figure 5 uses barycentric coordinates to display the three rows of $\bar{\boldsymbol{Q}}^{(i)}$ for each person. The points are colored red, green, and blue to correspond to rows (and thus, starting environments) 1, 2, and 3 of $\bar{\boldsymbol{Q}}^{(i)}$, respectively. Each row is an ordered triple containing the probabilities of transitioning to each environment, which we have mapped into a point of a two-dimensional ternary plot using the R package Ternary (Smith 2017). (The reduction from three to two dimensions is made possible by the fact that the three probabilities are constrained to add to one.) The three vertices of the ternary plot correspond to (clockwise starting at the top) the points (1, 0, 0), (0, 1, 0), and (0, 0, 1), at which there is probability 1 of transitioning to a specific environment. The side opposite each vertex is an axis along which there is constant probability 0 of transitioning into the environment corresponding to that vertex, and the lines parallel to each axis mark increasing probability of transitioning to the environment as they approach the vertex. To read one of the three transition probabilities associated with a given point,

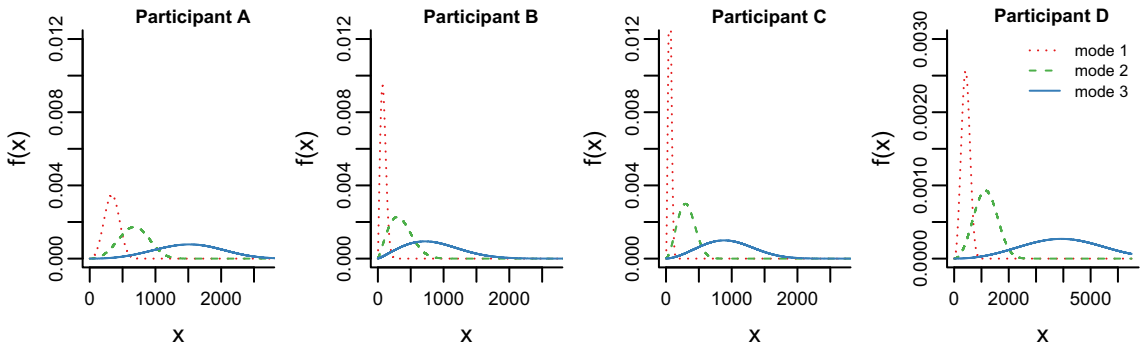


**Fig. 4** Monte Carlo estimates of the predictive densities for the three response modes. (The *x*-axis for participant D is shown on a different scale). The color scheme matches that of Fig. 3

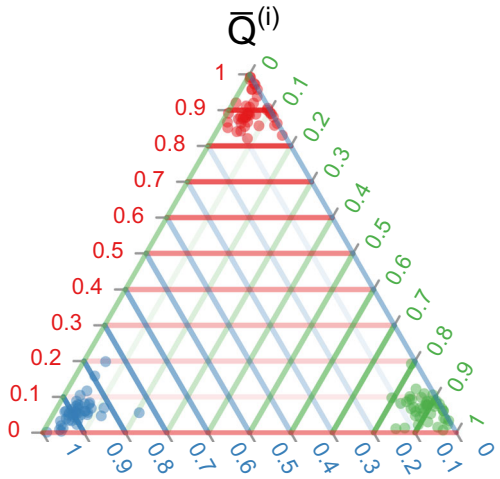


**Fig. 5** The posterior means of the rows of $\bar{\boldsymbol{Q}}^{(i)}$ for each person. Rows 1, 2, and 3 are plotted in red, blue, and green, respectively

trace a path parallel to a grid line of a given color to the axis label of the same color. For example, to read the probability of transitioning to environment 2, trace a path parallel to a green grid line to the green labels on the triangle. Figure 6 displays $\bar{\boldsymbol{P}}^{(i,e)}$, $e = 1,..., 3$ in the same way.

In Fig. 5, we see that within each environment, the rows of $\bar{\boldsymbol{Q}}^{(i)}$ for most people concentrate near the prior mean of the row. Their proximity to the vertex that corresponds to the starting environment indicates high probability of remaining in one's current environment in consecutive trials.

It is interesting to observe the points that fall very near one of the axes of the plot, along which transitions to one of the environments have probability 0. Many of the red points, row 1 of $\bar{\boldsymbol{Q}}^{(i)}$, fall near the blue axis, indicating that the posterior probability of transitioning from environment 1 to environment 3 is nearly zero. It is less typical for these red points to fall near the green axis; for most people, a transition to environment 2 is more likely than to environment 3 when starting in environment 1. We also see several green points (transition probabilities starting from environment 2) falling close to the blue axis and comparatively fewer near the red axis. In contrast, the blue points (transition probabilities starting from environment 3) are, for nearly all people, detached from both axes and from the vertex. These considerations highlight differences in how people move between the three environments: many are less likely to transition into environment 3, which promotes responses from the slowest RT distribution, than the other two environments. In contrast, when they are in environment 3, they do not exhibit a strong preference for transitioning into either one of the other two environments.

To summarize the typical behaviors across all participants we also calculated $\bar{\boldsymbol{Q}}$, which we use to denote the average of the posterior participant-specific mean TPMs. For each row $j$ and column $k$ of the TPM, we also calculated the average of the posterior participant-specific standard deviations of the $\boldsymbol{Q}^{(i)}_{j,k}$, which we denote by $s^{Q}_{j,k}$. The value of $s^{Q}_{j,k}$ reflects the typical posterior uncertainty in row $j$, column $k$ of $\boldsymbol{Q}^{(i)}$, ignoring across-participant variability. These values are shown in Fig. 7, with darker plotting shades corresponding to larger values of $\bar{\boldsymbol{Q}}_{j,k}$.

**Transitions Among Response Modes** The posterior means of the rows of the $\bar{\boldsymbol{P}}^{(i,1)}$, $\bar{\boldsymbol{P}}^{(i,2)}$, and $\bar{\boldsymbol{P}}^{(i,3)}$ matrices are plotted in Fig. 6. Using the same approach as in Fig. 5, the $e$-th plot shows each of the three rows of $\bar{\boldsymbol{P}}^{(i,e)}$, with rows 1, 2, and 3 represented in red, green, and blue, respectively. Color now represents the starting response mode rather than the environment.

In general, the points in all three plots concentrate near their prior means: as promoted by our prior specification, the typical person tends to favor transitions into response mode $e$ when in environment $e$. Several of the points corresponding to the selected participants stand out in the display. Participant B has unusual transition probabilities when in environment 1, as shown by the labeled points in the plot of $\bar{\boldsymbol{P}}^{(i,1)}$ (left panel). This person's green and blue labeled points show a probability of only 0.68 of moving to response mode 1 when in response mode 2, and only about 0.60 of moving to response mode 1 when

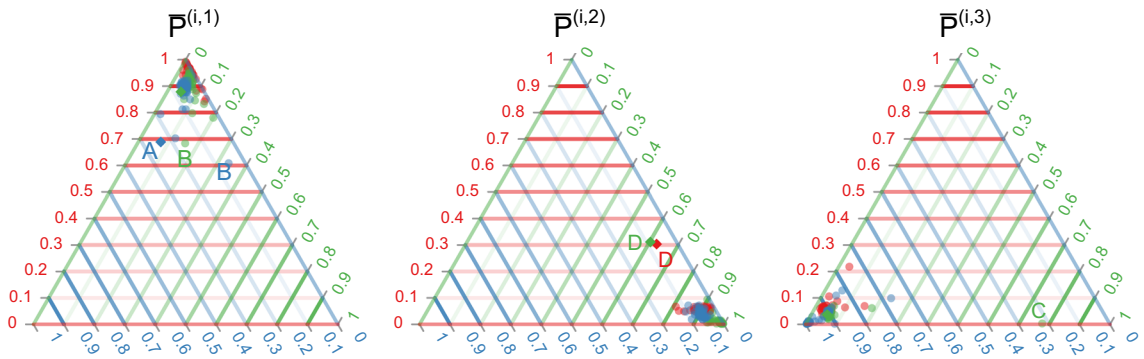


**Fig. 6** The panels show the posterior means of the rows of (from left) $\bar{\boldsymbol{P}}^{(i,1)}$, $\bar{\boldsymbol{P}}^{(i,2)}$, and $\bar{\boldsymbol{P}}^{(i,3)}$ for each participant. Rows 1, 2, and 3 are plotted in red, blue, and green, respectively

$\bar{Q}$

| | | |
|---|---|---|
| 0.90 (0.02) | 0.06 (0.02) | 0.05 (0.01) |
| 0.07 (0.02) | 0.89 (0.03) | 0.04 (0.02) |
| 0.06 (0.03) | 0.06 (0.04) | 0.88 (0.05) |

$\bar{P}1$

| | | |
|---|---|---|
| 0.95 (0.02) | 0.04 (0.02) | 0.01 (0.01) |
| 0.90 (0.08) | 0.06 (0.07) | 0.04 (0.04) |
| 0.87 (0.10) | 0.06 (0.06) | 0.07 (0.08) |

$\bar{P}2$

| | | |
|---|---|---|
| 0.06 (0.07) | 0.89 (0.09) | 0.05 (0.05) |
| 0.02 (0.01) | 0.97 (0.02) | 0.02 (0.01) |
| 0.04 (0.05) | 0.90 (0.09) | 0.06 (0.07) |

$\bar{P}3$

| | | |
|---|---|---|
| 0.06 (0.08) | 0.04 (0.05) | 0.89 (0.09) |
| 0.04 (0.05) | 0.08 (0.08) | 0.88 (0.09) |
| 0.02 (0.03) | 0.03 (0.03) | 0.95 (0.04) |

**Fig. 7** The across-participant average values of the TPMs, $\bar{\boldsymbol{Q}}$, $\bar{\boldsymbol{P}}^{\mathbf{1}}$, $\bar{\boldsymbol{P}}^{\mathbf{2}}$, and $\bar{\boldsymbol{P}}^{\mathbf{3}}$ are given by the displayed numbers and shade of squares, with high values corresponding to darker shades. The corresponding values of $\bar{s}^{\boldsymbol{Q}}_{j,k}$, $\bar{s}^{\boldsymbol{P}^1}_{j,k}$, $\bar{s}^{\boldsymbol{P}^2}_{j,k}$, and $\bar{s}^{\boldsymbol{P}^3}_{j,k}$ are shown in parentheses for all $j$, $k$

in response mode 3. Compared to the prior expectation and the other participants, this person shows less of a preference for moving to response mode 1 while in environment 1. Participant D stands out as unusual while in environment 2 (middle panel): when starting in response mode 1 or 2, the posterior probability of transitioning into response mode 2 is only about 0.60. Finally, in environment 3 (right panel), participant C has a surprisingly high posterior probability (0.78) of persisting in response mode 2 while in environment 3, which typically promotes transitions into response mode 3 instead. The unusual transition probabilities of some people are indicative of a person's tendency to sojourn in certain environments in unusual ways. These tendencies are further explored in the next section.

## Latent Process for Selected Participants

We estimated the latent process underlying each person's RT sequence by calculating, at each trial $t$, the environment/response mode pair having maximum a posteriori frequency. Here we present these estimates for participants A, B, C, and D. These people were chosen because their estimated latent processes were either similar to those of the other participants or atypical in interesting ways. Figure 8 shows the RT sequences for these participants with points colored according to the estimated response mode and background colored according to the estimated environment. The right panels show the estimates $\bar{\boldsymbol{Q}}^{(i)}$ and $\bar{\boldsymbol{P}}^{(i,e)}$.

**Participant A** The behavior of participant A is typical of people in this experiment, with a sequence showing distinct periods of fast, medium, and slow RTs. This feature of the data produces estimated environments that tend to persist for blocks of consecutive trials, within which most trials are estimated to arise from that environment's favored response mode. The diagonal elements of $\bar{\boldsymbol{Q}}^{(i)}$ are a little higher than their prior means of 0.90—the estimated environments are slightly more persistent ("sticky") than the prior expectation. The posterior estimates of $\bar{\boldsymbol{P}}^{(i,e)}$ are similar to the prior expectations with two exceptions: $\bar{\boldsymbol{P}}^{(i,1)}_{3,3} = 0.24$ is quite large, indicating a tendency to persist in response mode 3 even when in environment 1, and $\bar{\boldsymbol{P}}^{(i,3)}_{3,3} = 0.99$ captures an unusually strong preference for response mode 3 while in environment 3.

**Participant B** Participant B's responses are marked by a distinctive period of similar, moderate RTs in the first 180 trials of the experiment, which is captured in our model by environment 2. The large posterior mean of $\bar{\boldsymbol{Q}}^{(i)}_{2,2} = 0.96$ reflects the above-average "stickiness" of this environment that allows it to persist for many trials. Participant B also shows an unusually strong preference for response mode 2 while in environment 2; the large value of $\bar{\boldsymbol{P}}^{(i,2)}_{2,2} = 0.99$ makes transitions to a different response mode unlikely. Environment 1 is used to describe this person's less-frequent periods of fast RTs and permits easier transitions to response modes 2 and 3, as indicated by the probabilities in column 1 of $\bar{\boldsymbol{P}}^{(i,1)}$, which are lower than their prior expectations. In environment 3, this person strongly favors response mode 3.

**Participant C** The behavior of participant C is markedly different from that of a typical participant. There is a distinct changepoint around trial 450, where the person shifts from a period of moderate and slow responses to a period of moderate and very fast responses. The model uses environment 3 to describe the first period and environments 1 and 2 to capture the shifts between fast and moderate RTs in the second. In contrast to our prior expectation that people will favor response mode 3 while in environment 3, this person tends to use both response mode 2 and response mode 3. The unusual role of environment 3 results in an atypical estimated $\boldsymbol{P}^{(i,3)}$; since both response modes 2 and 3 tend to persist over consecutive trials, we see a high posterior probability on the diagonal elements $\bar{\boldsymbol{P}}^{(i,3)}_{2,2}$ and $\bar{\boldsymbol{P}}^{(i,3)}_{3,3}$, with only the latter being expected a priori.

**Participant D** The slowest RTs for this person are extreme in magnitude, often more than 4000 ms, and do not typically occur in consecutive trials. Further, there are unusually long periods in which the RTs do not appear to respond substantially to any changes in the experimental conditions. The estimated latent

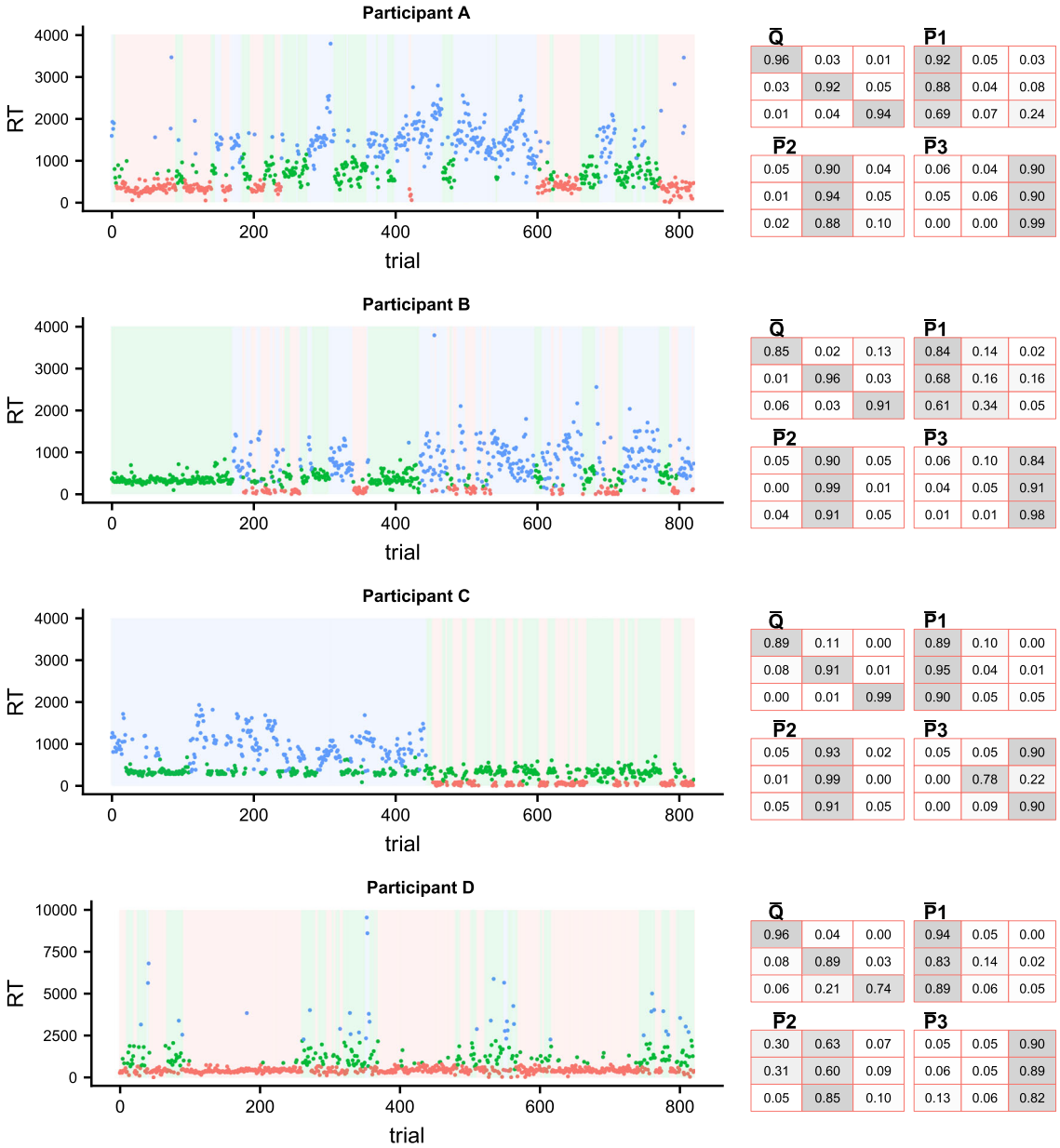


**Fig. 8** RT sequences for the selected participants. The plot background color corresponds to the estimated environment and the plotting color corresponds to the estimated response mode. The $y$-axis value is the observed RT at that trial. The matrices $\bar{\boldsymbol{Q}}^{(i)}$ and $\bar{\boldsymbol{P}}^{(i,e)}$ are shown to the right with darker shades of gray denoting higher values of the probabilities

process adjusts to accommodate these unusual features: the data show little evidence of periods favoring slow RTs, and so environment 3 is seldom used. Instead, most RTs for this person are estimated to be in environment 1, which describes the long periods of stable behavior and persists with mean posterior probability of $\bar{\boldsymbol{Q}}^{(i)}_{1,1} = 0.96$. Environment 2 describes the periods in which the fast, moderate, and slow RTs all tend to occur without a clear preference for one type. The estimated $\bar{\boldsymbol{P}}^{(i,2)}$ reflects this unusual behavior: the low expected posterior probabilities of transitioning to response mode 2 are consistent with an environment 2 that does not show strong preference for response mode 2 only.

The latent environments, as proposed in "A Bayesian Hierarchical HMM for RTs," are assumed a priori to represent periods of consecutive RTs that favor responses from a particular RT distribution. For people who respond as expected, such as participant A above, the posterior estimates are informative features about the three processes. For people who behave unusually, such as participant C above, the environments can adapt to describe the unusual trends in the data. These interesting participants are readily identified through unusual values in the person-specific posterior expected TPMs.

## Model Validation

We ignored the known experimental conditions (the distance of the target to aperture boundary) when we fit our model, relying instead on the hidden Markov structure to recover periods of shifting RTs. We now compare the estimated environments from the model to the true experimental conditions. The model we fit is deliberately ignorant of these conditions, as it is designed to pick up periods of shifting behavior in the data in the absence of explanatory covariate information (which is typically the case). A close correspondence between the estimated environments and true conditions would indicate that the participant's behavior aligns with the underlying experimental conditions and that the model can identify such an alignment, even though the experimental conditions are not explicitly accounted for.

We summarized the degree of correspondence for each person by calculating an overall similarity for person $i$ as $c_i = T^{-1}\sum_{t=1}^{T} I\left(\widehat{e}_t^i = e_t^i\right)$, where $\widehat{e}_t^i$ is the estimated environment for person $i$ at trial $t$, $e_i^t$ is the true experimental condition (as determined by the target-to-aperture distance for trial $t$), and $T$ is the total number of trials. Then, we calculate within-environment similarities $c_{ie} = \sum_{t:e_t^i=e} I\left(\widehat{e}_t^i = e\right) / \sum_{t=1}^{T} I\left(e_t^i = e\right)$, $e = 1, 2, 3$. The quantity $c_i$ is the proportion of trials for which the estimated environment matches the true experimental condition and $c_{ie}$ is the proportion of trials in condition $e$ for which the environment was indeed estimated to be equal to $e$. Figure 9 shows the values of $c_{i1}$, $c_{i2}$, $c_{i3}$, and $c_i$ for all participants. The similarities tend to be highest in condition 1 (red points), where the majority of people have similarities greater than 75%, and lowest in condition 3, where it was not unusual to see similarities below 50%. Among the participants with lower values of $c_i$, the high separation between red and blue points suggests that environment 1 is estimated too frequently and environment 3 is not estimated frequently enough.

In Fig. 10, we have plotted the RTs with the estimated environments for the previously discussed participants A and D, as well as the two participants whose overall similarity was the highest (called participant E) and lowest (called participant F) among the people in the study. The color of each point corresponds to the *true experimental condition* at that trial (in contrast to Fig. 8, where the color matches the estimated response mode). As in Fig. 8, the background is colored to match the estimated environment. Participant E, for whom overall similarity was 87%, has RTs that appear to come from three well-separated distributions and these closely reflect the true experimental conditions. For participant F, on the other hand, $c_i$ was only 30%. This person's RT sequence does not exhibit predictable changes corresponding to experimental condition, and the environments for this person instead capture a period of slower RTs with high variability (represented by environments 2 and 3) and a shift to more stable behavior in the latter half of the experiment (represented by environment 1).

Our model adapts flexibly to the differences between the behaviors of participants E and F. The clear separation among RT distributions for participant E corresponds closely to our prior expectation of behavior in this experiment. The estimated environments shift frequently to recover much of the information about the experimental conditions. In contrast, the predominant pattern in the data for participant F is a long-term trend of gradually quickening RTs. This participant does not appear to respond to the changes in difficulty of the task. In response to this unexpected behavior, the estimated environments provide a discrete representation of the longer-term trend by picking up on periods when the RT distributions appear to shift most clearly.

In a practical setting, if information about underlying conditions were available, we would not reserve it for model validation, but include it as a covariate in the model. In our application, for example, a fixed effect in the scale or shape of the Weibull distribution could be included to account for behavior that can be attributable to changes in the stimulus

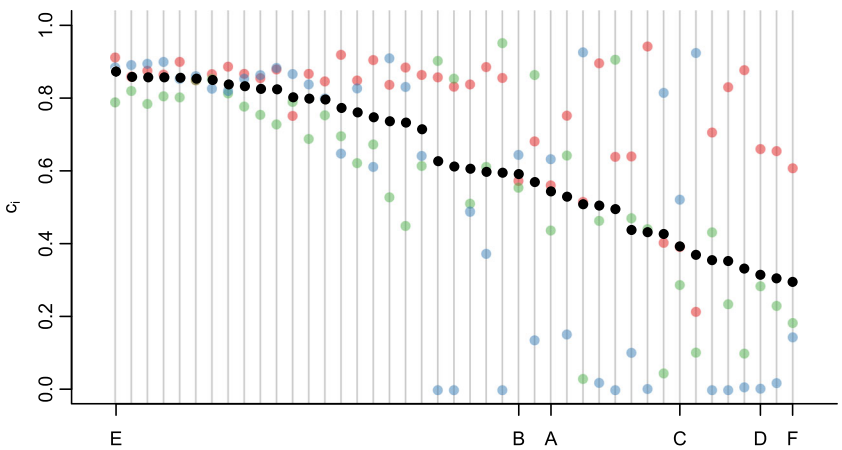


**Fig. 9** Values of the within-environment and overall similarities, $c_{i1}$, $c_{i2}$, $c_{i3}$, and $c_i$, shown for each participant in red, green, blue, and black, respectively. The participants are shown in order of descending $c_i$ to improve readability

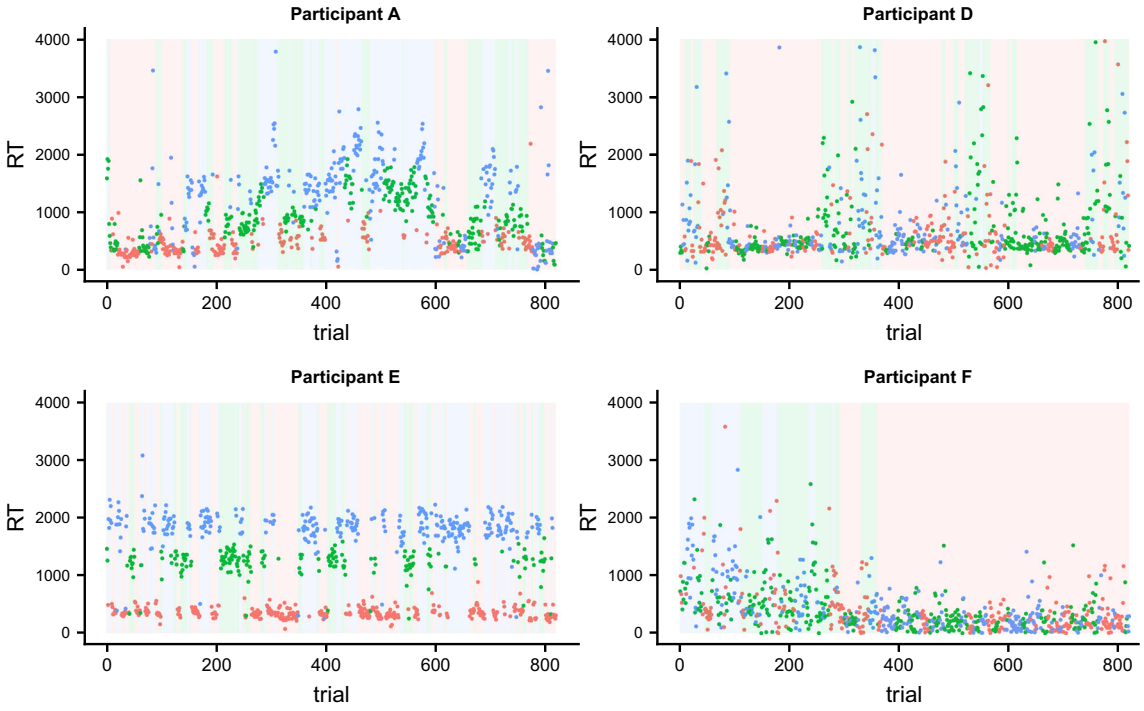


**Fig. 10** RT sequences for the selected participants. The plot background color corresponds to the estimated environment and the plotting color is the true experimental condition. The overall similarity values $c_i$ for participants A, D, E, and F are **0.54**, **0.31**, **0.87**, and **0.30**, respectively

distance. The environments in this setting would then capture shifts in the distribution of the residuals, which could correspond, for example, to periods of unexpected slowing due to external, unmeasured factors.

## Application to Wagenmakers' Data

Wagenmakers et al. (2004) designed a number of different experiments to investigate the presence of serial correlation in RT sequences. There were six people in each experiment.

We will focus on the "simple RT experiment," where each person was instructed to press a key right after observing one of the numerals 1, 2, 3, 4, 6, 7, 8, or 9 on a computer monitor. This task was repeated for 1048 trials in total without breaks. The first 24 "practice" trials were discarded. For the remaining 1024 trials, the RTs were recorded in ms for each person. To prevent fast anticipatory responses the researchers randomly manipulated the response-stimulus interval (RSI). Here we will study the "short" RSI condition, where RSI were uniformly generated between 200 and 801 ms. (There was another experiment carried out involving a longer RSI condition. The supplemental materials describe results of analyzing the data from this condition.)

Craigmile et al. (2010) fit a non-Gaussian mixture time series model to these RT data that includes a trend term to capture long-term variations in the response. Most people's RTs exhibited significant autocorrelation over trials even after accounting for a trend. Each person showed evidence of fast, average, and slow RTs, which the model accounted for using three mixture components fit to the log RTs. The analysis in Craigmile et al. (2010) does not consider the modeling of latent environments and response modes that might influence the distributional characteristics of RTs.

We applied our current modeling framework to these data to evaluate the impact of these elements on the analysis and to illustrate how our model can be used in a situation where the experimental conditions do not tend to trigger responses from three distinct distributions. In this situation, we use the three mixture components to capture responses from the fast, medium, and slow RT distributions.

The HMM was fit using the same priors as in the main experiment on all model parameters except for $\boldsymbol{\kappa}$, the hyperparameter determining the prior mean of the log scale parameters. We set $\boldsymbol{\kappa} = (4, 6, 8)^T$ to reflect the shorter overall magnitude of the RTs in this experiment. The subsequent results demonstrate that, although our model makes strong prior assumptions concerning the assumed structure of the latent process, the data still play a crucial role in forging the posterior features of said structure.

Figure 11 shows the estimated response modes and environments for the six participants in the short RSI condition. Unlike the participants in our experiment who for the most part occupied all three environments, these people are estimated to spend most of the experiment in environment 2. Subjects 2, 4, and 6 very seldom leave environment 2, with changes occurring only in occasional periods when several slow RTs

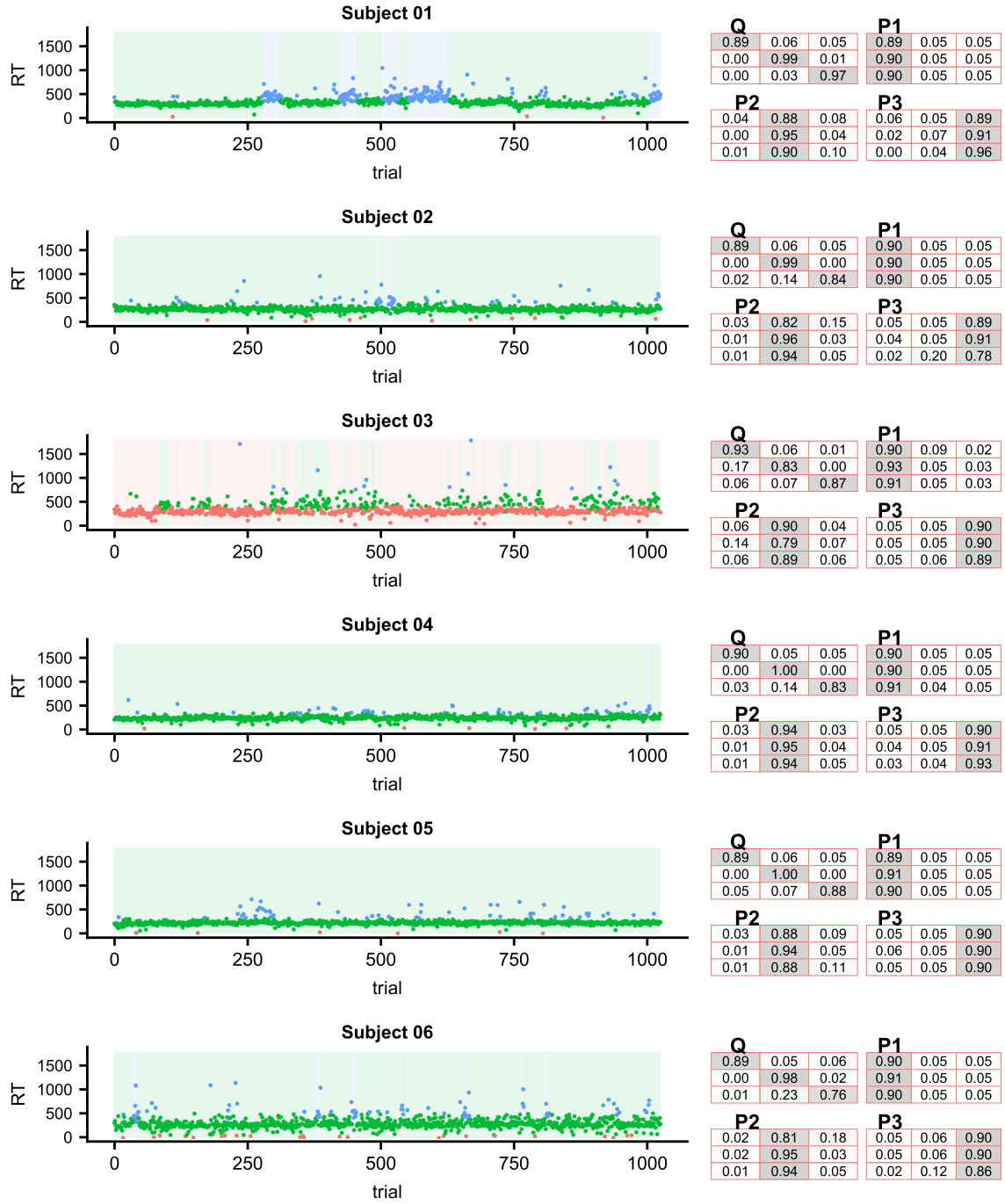


**Fig. 11** Estimated environments and response modes and posterior expected TPMs for the Wagenmakers data

occur over a short period. In these subjects, the posterior estimates $\bar{Q}^{(i)}$ have small (compared to the prior expectations) probabilities on the diagonal elements that correspond to the environments that are never entered. The behavior is different for subject 1, whose RT sequence has clear patterns of a trend in several places; this person enters environment 3 during several periods where the RTs slow slightly and more outliers occur. For subject 3, the most common estimated environment is 1, with comparatively frequent shifts into environment 2. The unusual estimates can likely be attributed to the influence of this person's slow outliers, which cause the slow distribution to shift to accommodate them. In the absence of shifts in RT distributions induced by the experimental conditions, the environments in our HMM adapt to describe trends in the data that could correspond to periods of distraction, fatigue, or inattention.

In contrast to the analysis of Craigmile et al. (2010), the HMM approach does not directly specify a smooth trend component in the model. Instead, it relies on the single hidden Markov chain to capture sporadic changes in the RT distributions through the response modes and long-term shifts using the environments. While the model of Craigmile et al. (2010) uses a three-component mixture to capture shifts in RT distributions separately from the trend, the HMM captures the long-term and short-term shifts jointly as a single latent process. To briefly illustrate the effect of these different modeling approaches, we obtained Monte Carlo samples of the posterior predictive median log RTs under both models. Figure 12 shows the RTs and the predictive medians estimated by the HMM (red lines) and the posterior predictive median log RTs estimated by the model of Craigmile et al. (2010) (navy lines).

Under the HMM, the predictive medians at most trials fall near the predictive median RT for one of the three response modes because the model puts high posterior probability on one of the response modes. For trials in which there is more posterior uncertainty regarding the latent response mode, the predictive median falls between these values, although this occurs in comparatively few trials. The result is a pattern of flat predictions for several trials followed by abrupt jumps when the response mode changes. In contrast, the predicted median RTs for the wavelet model of Craigmile et al. (2010) are different for each trial, varying smoothly in periods of moderate RTs and exhibiting larger shifts corresponding to extreme RTs. The two analyses nonetheless pick up on many of the same features: in areas where the smooth trend modeled by Craigmile et al. (2010) exhibits very pronounced peaks, we often see shifts in predicted RTs from the HMM corresponding to estimated shifts in the latent response modes. The HMM provides a coarse representation of only the most prominent trends in the RT sequences, while the model of Craigmile et al. (2010) tracks closely the observed RTs and picks up on smaller-scale variability.

## Prior Sensitivity

Informative priors are required on the TPMs to ensure posterior identifiability of the distinct mixture components. The structure of the prior TPMs, as shown in Fig. 2, embeds in our model our beliefs about what the latent environments represent. We investigated the sensitivity of the analysis to the prior by fitting the model with small adjustments to the prior means of the TPMs, which determine the expected nature of the latent process, and to the degree of concentration about the prior mean. In general, we have found that the estimated response modes and environments are robust to small changes in the prior mean TPMs and the level of prior concentration;

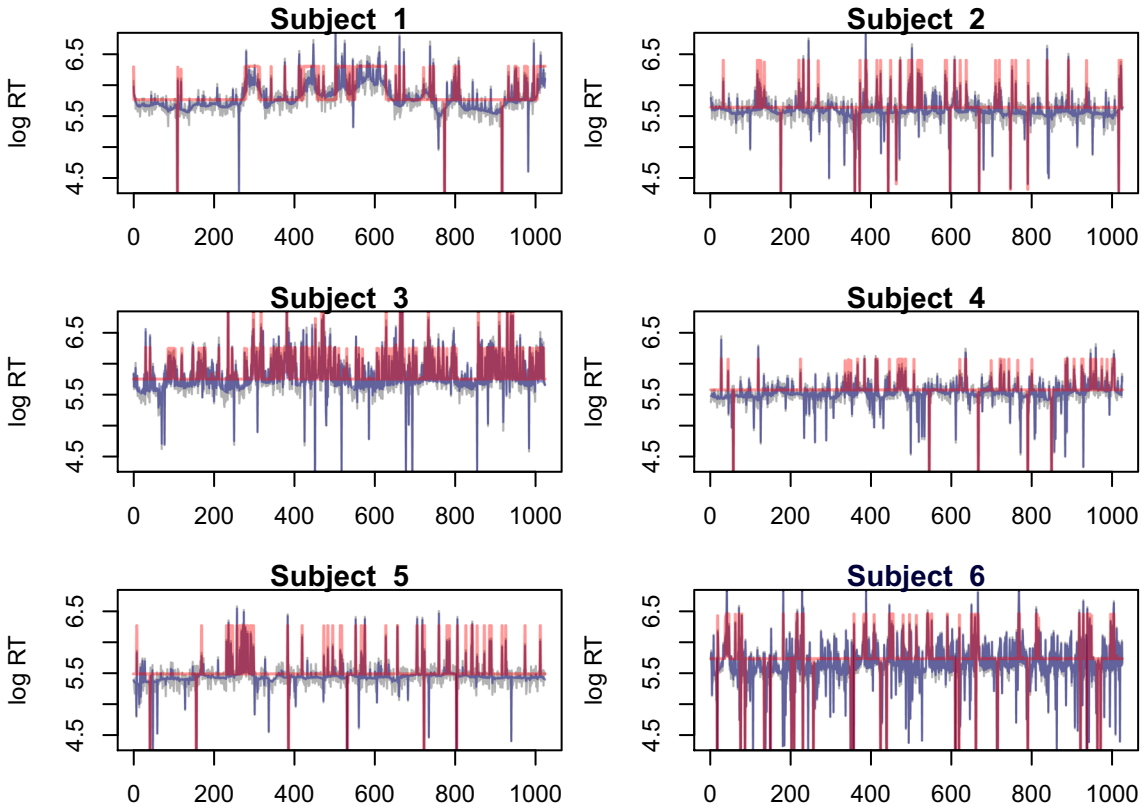


**Fig. 12** Observed log RTs for the Wagenmakers data (gray lines) and posterior predictive median log RTs under the HMM (red lines) and wavelet model (navy lines)

however, the estimated environments are sensitive to substantial changes in the prior mean TPMs. Further, we have found that the sensitivity is greater in the posterior TPMs than in the estimated latent states. This is because a large number of transitions must be observed in order to overcome the prior expectation for a given transition, and many transitions occur seldom in the data (such as transitions from response mode 1 to response mode 3 while in environment 2).

## Conclusions and Discussion

We developed a simple hierarchical structure to identify and isolate mixture components that we assume to be associated with a person's unobserved, underlying mental state. We used a two-tiered HMM to distinguish between different response modes (that attempt to capture changes in cognitive RT distributions) and different environments (that describe how people transition between different response modes). We applied our HMM to data from a detection experiment designed to influence the RT distribution and we demonstrated that the model fits those data well.

Our detection experiment serves as a proof-of-concept that we can use the hierarchical structure to identify different mixture components and differences between people. The model is also appropriate for data generated under experimental settings that, while varying over time, induce transitions in the cognitive mode that processes the experimental stimulus.

The application to the Wagenmakers data illustrates the flexibility of the model, which remains appropriate in situations where the experimental design is not intended to induce transitions between cognitive modes. In cases where there is little change in a person's mode of behavior, the model readily adapts by using fewer than three environments. In addition, the environments serve as an effective device to capture trends that manifest over time.

Our approach offers an alternative to direct modeling of a continuous, non-stationary trend as in our previous work (Craigmile et al. 2010; Kunkel et al. 2019), offering instead a coarse representation of periodic changes in behavior. In other modeling settings, theoretical or practical considerations may lead to preference for a continuous trend model to describe the same patterns, arising perhaps from parameters that vary over time. These two approaches have been explored in the context of mind-wandering (Hawkins et al. 2015, 2017), where the type of latent construct is closely tied to alternate theories of cognition. In future work, the HMM could be used to investigate the evidence in favor of a discrete representation of latent states.

In many applications of this methodology, the latent states will correspond to unobserved mental states such as attention/inattention or guessing/not guessing. The model could be applied to data from experimental studies that seek to place the participant in a different mental state (see Smallwood and Schooler 2015 for a discussion of the challenges of this type of manipulation) and collect information for validation either through self-reporting or by tracking external characteristics such as eye movement or pupil dilation (Foulsham et al. 2013; Franklin et al. 2013; Dillard et al. 2014). Expected behaviors within different states could then be incorporated into different priors on the component-specific parameters or TPMs.

The methodology is not tied to the assumption that there are 3 latent environments and 3 response modes. The forward-backward algorithm used to fit the model (described in the supplementary materials) can be extended to handle an arbitrary number of states in the HMM, and the number of environments need not match the number of response modes. Possible extensions would encompass models that can learn from the data the number of latent states that are needed for a given experimental setting. Such models would enable the investigator to determine, for example, if more environments are needed when the level of difficulty of the task increases.

Currently, we do not know if the number of environments and response modes should be the same for each person under study. To resolve this uncertainty, we might consider several combinations of environments/response modes and compare the resulting models using an appropriate model selection criterion as suggested by Frühwirth-Schnatter (2006), or use a more automatic procedure such as those based on hierarchical Dirichlet processes (Beal et al. 2001; Teh et al. 2005) to choose the number of hidden states. It is reassuring, however, that even in its current implementation the methodology can easily adapt to the data and ignore unnecessary latent states simply by not visiting them.

There are many potential applications to patient populations. Building HMMs whose parameters vary over individuals, we can use posterior estimates of the latent states to identify individuals who are, for example, more prone to distraction, less sensitive to environmental conditions, and so forth. Posterior inference on the parameters of the RT distributions can further distinguish between participants who behave as expected and those who deviate from our prior expectations. Potentially, this can lead to more refined diagnostic tools for conditions such as ADHD, where a person is not only classified as having or not having the given condition but also quantitatively characterized in terms of the specific behavioral and cognitive traits that lead to the diagnosis (see e.g., Thaler et al. 2013; Kofler et al. 2017; Nigg et al. 2005).

**Acknowledgments** This material is based upon work supported by the National Science Foundation under grant nos. SES-1024709, SES-1424481, and DMS-1407604.

## References


Bastian, M., & Sackur, J. (2013). Mind wandering at the fingertips: automatic parsing of subjective states based on response time variability. *Frontiers in Psychology, 4*, 573.

Beal, M. J., Ghahramani, Z., & Rasmussen, C. E. (2001). The infinite hidden Markov model. In *Proceedings of the 14th International Conference on Neural Information Processing Systems: Natural and Synthetic, NIPS'01* (pp. 577–584). MIT Press.

Bhar, R., & Hamori, S. (2004). *Hidden Markov models: applications to financial economics*. New York: Springer.

Borst, J. P., & Anderson, J. R. (2015). The discovery of processing stages: analyzing EEG data with hidden semi-Markov models. *NeuroImage, 108*, 60–73.

Craigmile, P. F., Peruggia, M., & Van Zandt, T. (2010). Hierarchical Bayes models for response time data. *Psychometrika, 75*, 613–632.

Craigmile, P. F., Peruggia, M., & Van Zandt, T. (2012). A Bayesian hierarchical model for response time data providing evidence for criteria changes over time. In M. C. Edwards & R. C. MacCallum (Eds.), *Current issues in the theory and application of latent variable models* (pp. 42–61). New York: Taylor and Francis.

Dillard, M. B., Warm, J. S., Funke, G. J., Funke, M. E., Victor S. Finomore, J., Matthews, G., Shaw, T. H., and Parasuraman, R. (2014). The sustained attention to response task (SART) does not promote mindlessness during vigilance performance. Human Factors, 56:1364–1379.

Falmagne, J. (1965). Stochastic models for choice reaction time with applications to experimental results. *Journal of Mathematical Psychology, 2*, 77–124.

Falmagne, R. (1968). A direct investigation of hypothesis-making behavior in concept identification. *Psychonomic Science, 13*, 335–336.

Foulsham, T., Farley, J., & Kingstone, A. (2013). Canadian journal of experimental psychology/revue canadienne de psychologie expérimentale. *Human Factors, 61*, 51–59.

Franklin, M. S., Broadway, J. M., Mrazek, M. D., Smallwood, J., & Schooler, J. W. (2013). Window to the wandering mind: pupillometry of spontaneous thought while reading. *Quarterly Journal of Experimental Psychology, 66*, 2289–2294.

Frühwirth-Schnatter, S. (2006). *Finite mixture and Markov switching models*. New York: Springer.

Gales, M., & Young, S. (2007). The application of hidden Markov models in speech recognition. *Foundations and Trends in Signal Processing, 1*, 195–304.

Gelman, A. (2007). Comment: Bayesian checking of the second levels of hierarchical models. *Statistical Science, 22*, 349–352.

Hawkins, G., Mittner, M., Boekel, W., Heathcote, A., & Forstmann, B. (2015). Toward a model-based cognitive neuroscience of mind wandering. *Neuroscience, 310*, 290–305.

Hawkins, G. E., Mittner, M., Forstmann, B. U., & Heathcote, A. (2017). On the efficiency of neurally-informed cognitive models to identify latent cognitive states. *Journal of Mathematical Psychology, 76*, 142–155 Model-based Cognitive Neuroscience.

Juang, B. H., & Rabiner, L. R. (1991). Hidden Markov models for speech recognition. *Technometrics, 33*, 251–272.

Kim, S., Potter, K., Craigmile, P. F., Peruggia, M., & Van Zandt, T. (2017). A Bayesian race model for recognition memory. *Journal of the American Statistical Association, 112*, 77–91.

Kofler, M. J., Sarver, D. E., Spiegel, J. A., Day, T. N., Harmon, S. L., & Wells, E. L. (2017). Heterogeneity in ADHD: neurocognitive predictors of peer, family, and academic functioning. *Child Neuropsychology, 23*, 733–759.

Kunkel, D., Potter, K., Craigmile, P. F., Peruggia, M., & Van Zandt, T. (2019). A bayesian race model for response times under cyclic stimulus discriminability. *The Annals of Applied Statistics, 13*, 271–296.

Lindsen, J. P., & de Jong, R. (2010). Distinguishing between the partial-mapping preparation hypothesis and the failure-to-engage hypothesis of residual switch costs. *Journal of Experimental Psychology: Human Perception and Performance, 36*, 1207–1226.

Logan, G. D. (1988). Toward an instance theory of automatization. *Psychological Review, 95*, 492–527.

Logan, G. D. (1992). Shapes of reaction-time distributions and shapes of learning curves: a test of the instance theory of automaticity. *Journal of Experimental Psychology. Learning, Memory, and Cognition, 18*, 883–914.

Majoros, W. (2007). *Methods for computational gene prediction*. Cambridge: Cambridge University Press.

Meyer, D. E., Osman, A. M., Irwin, D. E., & Yantis, S. (1988). Modern mental chronometry. *Biological Psychology, 26*, 3–67.

Molenaar, D., & Boeck, P. (2018). Response mixture modeling: accounting for heterogeneity in item characteristics across response times. *Psychometrika, 83*, 279–297.

Nigg, J. T., Willcutt, E. G., Doyle, A. E., & Sonuga-Barke, E. J. (2005). Causal heterogeneity in attention-deficit/hyperactivity disorder: do we need neuropsychologically impaired subtypes? *Biological Psychiatry, 57*, 1224–1230.

Ollman, R. (1966). Fast guesses in choice reaction time. *Psychonomic Science, 6*, 155–156.

Palmer, E. M., Horowitz, T. S., Torralba, A., & Wolfe, J. M. (2011). What are the shapes of response time distributions in visual search? *Journal of experimental psychology: Human perception and performance, 37*, 58â€“71.

Peruggia, M., Van Zandt, T., & Chen, M. (2002). Was it a car or a cat I saw? An analysis of response times for word recognition. In *Case Studies in Bayesian Statistics* (Vol. 6, pp. 319–334). New York: Springer.

Rabiner, L. R. (1989). A tutorial on hidden Markov models and selected applications in speech recognition. In *Proceedings of the IEEE* (Vol. 7, pp. 257–286).

Ranger, J., Wolgast, A., & Kuhn, J. (2018). Robust estimation of the hierarchical model for responses and response times. *British Journal of Mathematical and Statistical Psychology, 72*, 83–107.

Rouder, J. N., Sun, D., Speckman, P. L., Lu, J., & Zhou, D. (2003). A hierarchical Bayesian statistical framework for response time distributions. *Psychometrika, 68*, 589–606.

Rouder, J. N., Lu, J., Speckman, P., Sun, D., & Jiang, Y. (2005). A hierarchical model for estimating response time distributions. *Psychonomic Bulletin and Review, 12*, 195–223.

Sarkar, A., Chabout, J., Macopson, J. J., Jarvis, E. D., & Dunson, D. B. (2018). Bayesian semiparametric mixed effects Markov models with application to vocalization syntax. *Journal of the American Statistical Association, 113*(524), 1515–1527.

Sederberg, P. (2016). SMILE: State Machine Interface Library for Experiments. Retrieved from https://github.com/compmem/smile/.

Smallwood, J., & Schooler, J. W. (2015). The science of mind wandering: empirically navigating the stream of consciousness. *Annual Review of Psychology, 66*, 487–518.

Smith, M. R. (2017). Ternary: an R package for creating ternary plots. Zenodo. doi: https://doi.org/10.5281/zenodo.1068996.

Teh, Y. W., Jordan, M. I., Beal, M. J., & Blei, D. M. (2005). Sharing clusters among related groups: hierarchical Dirichlet processes. In L. K. Saul, Y. Weiss, & L. Bottou (Eds.), *Advances in Neural Information Processing Systems 17* (pp. 1385–1392). MIT Press.

Thaler, N. S., Bello, D. T., & Etcoff, L. M. (2013). WISC-IV profiles are associated with differences in symptomatology and outcome in children with ADHD. *Journal of Attention Disorders, 17*(4), 291–301.

Tokuda, K., Nankaku, Y., Toda, T., Zen, H., Yamagishi, J., & Oura, K. (2013). Speech synthesis based on hidden Markov models. *Proceedings of the IEEE, 101*, 1234–1252.

Vandekerckhove, J., Tuerlinckx, F., and Lee, M. (2008). A Bayesian approach to diffusion process models of decision-making. Pages 1429–1434. Cognitive science society; Austin, TX.

Wagenmakers, E.-J., Farrell, S., & Ratcliff, R. (2004). Estimation and interpretation of 1/*f* noise in human cognition. *Psychonomic Bulletin & Review, 11*, 579–615.

Wang, Z., Chen, Y., & Li, Y. (2004). A brief review of computational gene prediction methods. *Genomics, Proteomics & Bioinformatics, 2*, 216–221.

Yantis, S., & Meyer, D. E. (1988). Dynamics of activation in semantic and episodic memory. *Journal of Experimental Psychology: General, 117*, 130.

Yellott, J. I. (1971). Correction for fast guessing and the speed-accuracy tradeoff in choice reaction time. *Journal of Mathematical Psychology, 8*, 159–199.

Yoon, B.-J. (2009). Hidden Markov models and their applications in biological sequence analysis. *Current Genomics, 10*, 402–415.

**Publisher's Note** Springer Nature remains neutral with regard to jurisdictional claims in published maps and institutional affiliations.